Partial Discharge Characterization in a Defect Subjected to HVDC Cable Operating Conditions

A. Imburgia, *Member IEEE*, G. Rizzo, G. Ala, *Senior Member IEEE*, T. J. Å. Hammarström, Y. V. Serdyuk, *Member IEEE,* A. Di Fatta*, Student Member IEEE*, P. Romano, *Senior Member IEEE*

***Abstract*—In this work, the role of the electric conductivity on variations of the PD phenomenon in XLPE insulation under DC stress is investigated and demonstrated. To enable this investigation, a new experimental setup simulating the insulating layer of a cable with an embedded air void defect and subjected to a DC stress and temperature has been proposed. The setup consists of two flat specimens connected in series. One of them is heated while the other one, that contains the defect, is kept at ambient temperature. Consequently, the electric fields induced by the externally applied DC stress differ between the two specimens. In this way, a conductivity variation between two dielectric layers is obtained. To facilitate the usage of this method, a new simulation model related to the proposed experimental setup has also been developed. The model is an extension of the three-capacitor model, in which variable resistors are introduced. Both simulation and experimental results indicate that the introduced discrete thermal gradient results in higher conductivity values and enhanced PD activity.**

***Index Terms*— HVDC, Partial Discharge, Simulation Model, Conductivity variation, Thermal Gradient.**

I. INTRODUCTION

INSULATING materials employed in high voltage systems are exposed to different electrical degradation factors dependent on specific application [1]-[3]. In most cases, the reduction of insulation lifetime is attributed to the presence and intensity of Partial Discharges (PDs). This phenomenon typically occurs in defects constituted by an air bubble located within the cable dielectric layer. They can be generated during the cable manufacturing process or caused by mechanical stress (e.g. bending) to which the cable is subjected during installation. In addition, air void defect can also be promoted from thermal stress (due to the different coefficients of thermal expansion of the materials constituting the cable) to which the cable is subjected during the normal operating condition.

The PD phenomenon has been widely investigated and the obtained results are well consolidated, especially for AC powered systems [4]. In contrast, PD phenomena under DC stress still needs to be further investigated despite of the continuous progress in this area.

The challenges in studying PD phenomena under DC stress appear due to the fact that the initiation and the number of PDs strongly depend on the applied waveform, especially on slopes at which the voltage rises and/or drops. In steady state conditions and without a thermal gradient, the number of PDs may be very low and their initiation often requires relatively high voltage magnitudes. The triggering of PD sometimes occurs very close to dielectric breakdown voltage, without any evidence of direct correlation between the two phenomena [5]-[6]. In addition, the effect of the thermal gradient plays an important role affecting conditions for triggering of PDs as well as their Repetition Rate (PDRR) [7].

Recently, a paper was published aimed at overcoming some problems related to the detection of PD under DC stress [8], as well as other studies focused on the effect of the thermal gradient on the space charge accumulation phenomenon which, in turn, influences the PD behaviour [9]-[10]. However, still more work is needed to explore specific features of the PD phenomenon under DC voltage.

In [7] the authors evaluate the PD behavior in a model cable with an air void defect subjected to the DC stress and thermal gradient. However, in that previous experimental test, the PD phenomenon was influenced not only by the temperature gradient (which generates a different electric field distribution due to the different conductivity gradient) but also by the thermal diffusion that affect the entire cable thickness and, in turn, the air void defect.

In the light of this, the aim of the present work, which is an extension and a deepening of the previously published paper [11], is to highlight the effect of the electric conductivity distribution in the insulation on initiation of PDs under DC stresses and temperature differences. It is anticipated that this effect may be essential because the PD phenomena is driven by

This paragraph of the first footnote will contain the date on which you submitted your paper for review, which is populated by IEEE. It is IEEE style to display support information, including sponsor and financial support acknowledgment, here and not in an acknowledgment section at the end of the article. This work was realized with the co-financing from European Union – FSE, PON Research and Innovation 2014-2020 – DM 1062/2021. *(Corresponding author: A. Imburgia).*

A. Imburgia, P. Romano, A. Di Fatta and G. Ala are with the L.E.PR.E. HV Laboratory, Department of Engineering, University of Palermo, Palermo, Italy. (e-mail: antonino.imburgia01@unipa.it, pietro.romano@unipa.it, alessio.difatta@unipa.it, guido.ala@unipa.it).

G. Rizzo is with EOSS, Prysmian Group, Milan, Italy. (e-mail: giuseppe.rizzo@prysmiangroup.com).

T. J. Å. Hammarström and Y. V. Serdyuk are with the Chalmers University of Technology, Göteborg, Sweden. (e-mail: thomas.hammarstrom@chalmers.se, yuriy.serdyuk@chalmers.se).

the electric field within a void in the material, which is related to the charge distribution over the entire insulation thickness. Moreover, temperature variations within the material influence the injection, motion, trapping and de-trapping of space charges. As demonstrated by several studies, the electric field inside a cavity depends on both the absolute value and the gradient of the temperature [6-7]. Whilst the former affects the ratio between the gas and dielectric conductivities in a proximity of the defect, the latter drives the electric field in the dielectric near the cavity. In order to highlight the role of the temperature gradient in enhancing the PD activity under DC stress, the study described in this work has been structured in such a way to exclude the role of the temperature variation near the defect. This has been achieved by means of a novel setup used to carry out experiments applying a controlled temperature difference to a couple of samples keeping the defected one always at room temperature. This experimental setup for the investigation of PD phenomena under DC stress is described in Section II. The results of the two experiments elaborating the temperature influence of the healthy sample are described in Section III. To better understand the role of the physical parameters influencing the phenomenon, a novel circuital model has been developed. This model is described in Section IV whilst the results of the simulations are reported in Section V. Finally, the conclusions complete the article.

II. Specimen Under Test and Measurement Setup

In the present study, instead of the continuous gradual temperature variation in a cable insulation, two regions with distinctively different temperatures are considered which mimic the layer of the material close to the heated conductor and the external layer, as displayed in Fig. 1a. Therefore, the continuous temperature gradient typically observed in a loaded HVDC cable has been introduced in a discrete manner, by means of a new measurement setup shown in Fig.1b. In Fig. 2 a schematic representation of the measurement setup focused on the structure of the specimens is reported.

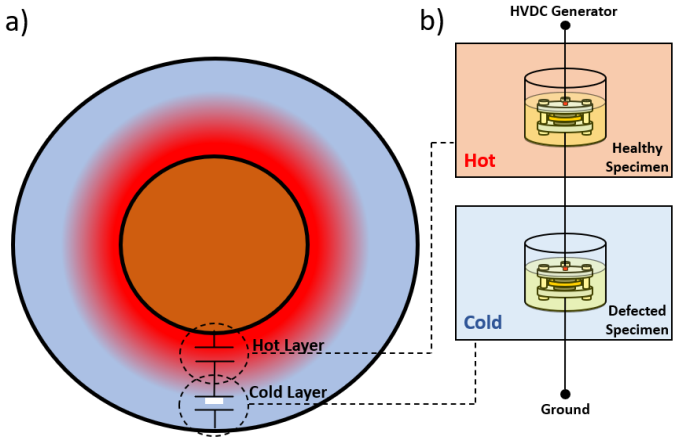

Fig. 1. a) Cable section in presence of thermal gradient and an air void defect. b) The arranged measurement setup composed of two specimens connected in series and immersed in two different tanks containing mineral oil.

The purpose of this discretization is also to exclude the role of the absolute temperature and to investigate only the impact of the temperature difference on the PD phenomenon.
The experimental setup consists of two specimens placed in series to each other and stressed by a DC voltage. One of the two specimens is made of a single XLPE layer with diameter equal to 40 mm and thickness 0.5 mm. The other specimen, instead, is composed by two layers of XLPE material both with diameter 40 mm and thickness 0.3 mm. In one layer of this specimen a 4 mm wide and 0.3 mm thick hole has been created to reproduce an air void defect. Both specimens, placed between two metallic electrodes, have been immersed in two different containers containing mineral oil. To avoid unwanted air bubbles as well as the penetration of the oil inside the air void constituting the defect, silicone grease was spread in the surfaces of the XLPE layers before tightening the specimen. The healthy specimen, simulating the inner part of the dielectric layer (near the cable core), is immersed in heated mineral oil, as shown in Fig. 3a. The heating of the mineral oil is realized by means of a temperature-controlled resistor which value is controlled automatically by a PT100 sensor. The specimen with the air defect, which simulates the outer part of the dielectric layer (colder in respect to the inner part), is immersed in oil kept at room temperature for all the tests. For the monitoring of the PD activity, the Pry-Cam wireless PD sensor has been adopted. It has been positioned in front of the defected specimen, as illustrated in Fig. 3b.

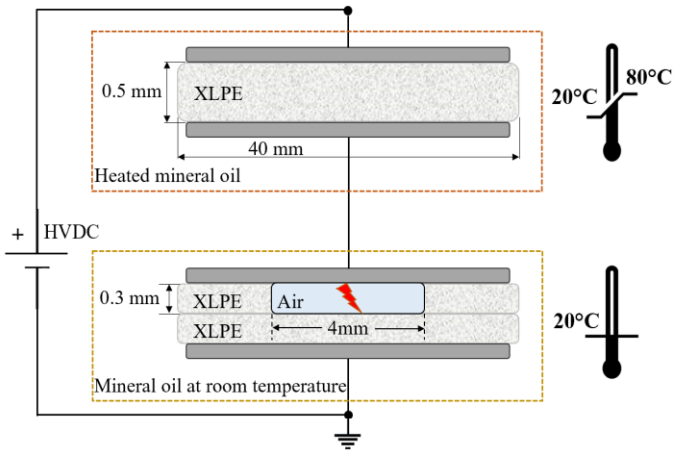

Fig. 2. The schematic representation of the measurement setup focused on the structure of the specimens.

As previously reported, the main purpose of this work is to highlight the role of the temperature gradient and, in turn, of the electric field distortion due to the conductivity variation, in the inception of PD phenomenon under DC stress. Based on this, “hot” (inner part of the insulating layer) and “cold” (outer part of insulating layer) specimens are only the discrete representation of a temperature gradient inside a cable. For this reason, is not important the exact position of the void inside the “cold” specimen but rather that the void is located in the “colder” part of the setup. The choice to select a cavity in contact with a metal electrode was done in order to have a lower

PD Inception Voltage (PDIV) and a higher current promoted by the "hot" specimen.

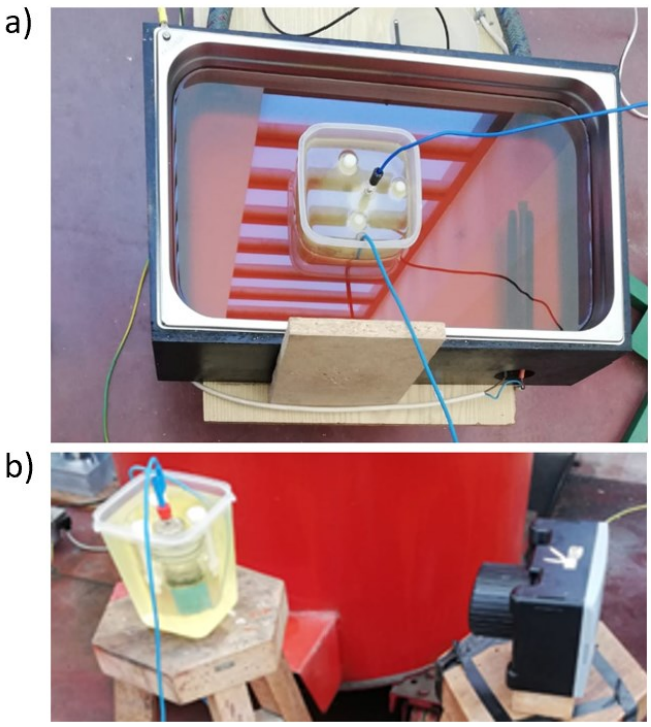

Fig. 3. a) Photograph of the healthy specimen immersed in heatable mineral oil. b) Photograph of the specimen containing the artificial defect and immersed in mineral oil at room temperature. In the photo the Pry-Cam used for the detection of PDs.

III. Test Procedure and Measurement Results

To observe the influence of temperature variation and respectively the effect of the conductivity variation on PD activity under DC stress, two different tests have been performed. The first test was conducted without introducing a temperature difference. Therefore, both specimens in Fig. 2 were kept at room temperature 20 °C. In the second test, a temperature difference was introduced and the temperature of the mineral oil, where the healthy specimen was immersed, was increased to 80 °C whereas the vessel with oil and immersed specimen containing the defect remained at 20 °C.

The shape of the applied test voltage used in both cases is shown in Fig. 4. The voltage of 10 kV magnitude was applied from the start of the tests for 6 minutes. Then, it was increased to 15 kV for further 4 minutes. Finally, the voltage was raised to 20 kV at 10 minutes and was kept at this magnitude for 6 minutes. In the last part of the tests, from minutes 16 to 17, the applied voltage magnitude was reduced to 0 kV. During this procedure, the time between two successive voltage levels was kept within a maximum of one second.

During the whole time of the test, from 0 to 17 mins, the PD activity has been monitored and the results are reported and discussed in the next sections.

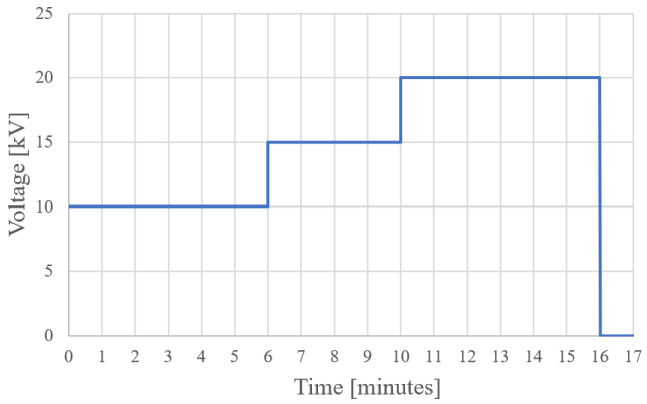

Fig. 4. The variation of the applied test voltage.

A. PD Detection at Room Temperature

In the first test, both specimens were maintained at the same temperature of 20°C.

In the first 5 mins of the voltage application, no PD events were observed. Then, some discharges during the increase of the voltage level from 10 to 15 kV (at 6 mins) and from 15 to 20 kV (at 10 mins) have been detected. At 8 mins, one single PD has been observed. Further, when the applied voltage was maintained at the constant value of 20 kV (from 10 to 16 min.), a greater number of PDs was registered. The signal from a single PD pulse detected in this time interval is shown in Fig. 5.

Its shape is similar to that of an internal PD pulse presented in [12]. To confirm the presence of internal discharges, this pulse shape was compared with PD pulses detected in the previously conducted experiment with the same specimen exposed to AC stress.

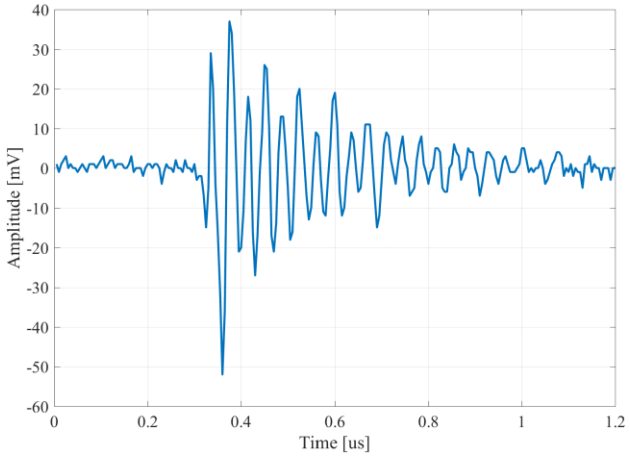

Fig. 5. Acquired PD pulse during the test with both specimens kept at room temperature.

In the test, pulses with waveforms different from that of the typical PD events have also been acquired and filtered with an appropriate denoising software. After removing unwanted signals, the time trend of the PDRR considered as the occurring number of PD events per minutes, has been calculated and is reported in Fig. 6. As can be seen, the intensity of PDs is significant when the voltage is kept at the stationary value of 20 kV (from 10 to 16 mins). The maximum PDRR value equal to

6 events/minutes is reached at 12 mins. After that, the detected PDs are reduced at 2 events/min at 13 and 15 minutes, and only 1 event/min at 14 mins. The last discharge is detected at 17 mins, which corresponds to the time in which the applied voltage is reduced at 0 V.

To complete the analysis of PD behavior, the amplitude of each PD pulse has been registered and is reported in Fig. 7.

It shows that a majority of PDs resulted in the average amplitude of around 40 mV and some discharges with the amplitude in the range from 70 to 100 mV. By analyzing the amplitude of each acquired PD pulse, unlike what established by the authors in the previous paper [11], it was found by studying the PD distribution and frequency content in detail, only the discharges with an amplitude with magnitude up to 40 mV (such as all the PD events in the histogram of Fig. 6) are found related to the internal PDs as obtained in the discharge recognition analysis carried out in [13]. All other discharges, those with greater amplitude, are signals due other factors, e.g. noise or corona discharges. For these reasons all the detected discharges with magnitudes in the range 70-100 mV have been filtered out and are not considered in the present PD analysis.

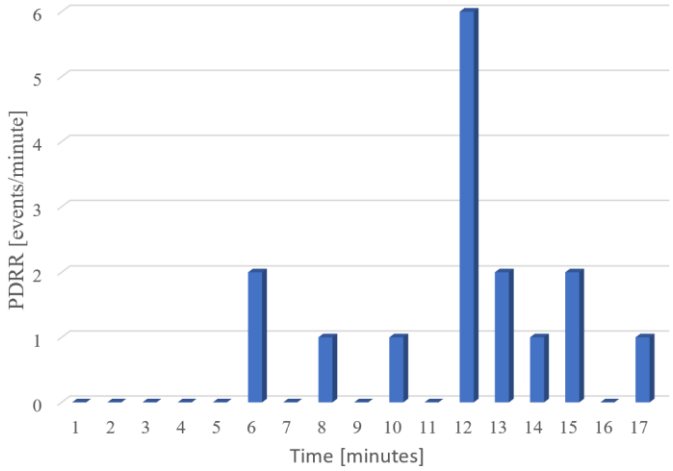

Fig. 6. Trend of the PDRR related to the experimental test in which both specimens are kept at room temperature.

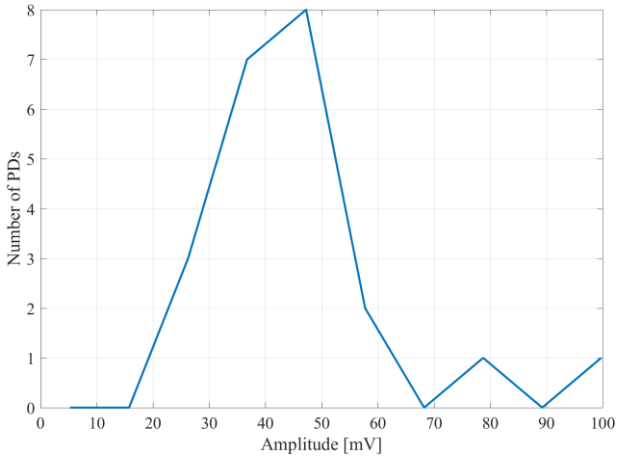

Fig. 7. Amplitude distribution of the PD signals acquired in the test with both specimens kept at room temperature.

B. PD Detection Under Temperature Difference

In the second test, the temperature of the healthy specimen was increased to 80 °C, while the specimen containing the defect was maintained at 20 °C. This temperature difference affected the internal voltage division and the electric field distribution thus introducing different conductance between the samples. The same DC voltage as used in the previous experimental test (Fig. 4) was applied.

The choose of 80°C of the hot specimen is useful to obtain a significant number of internal PD by applying a voltage magnitude that does not allow a high corona discharge activity in the measurement setup connections. The need to detect a significant number of discharges, at least an order of magnitude higher than the measurement uncertainty, is also useful for better evaluating the reliability of the implemented dielectric conductivity model that will be explained in the next Section.

However, the only PD parameter that is influenced by the high temperature imposed in the healthy specimen is the highest number of PD pulses detected, in respect to the case in which both specimens are at the same temperature.

In this case, the most intense PDs were observed when the stress magnitude reached 20 kV (between 11 to 16 mins after the test started). The shapes of the detected PD pulses, excluding the spurious signals eliminated by the denoising process, are very similar to each other and confirm the presence of internal discharges as the magnitude and the frequency content remain similar to the previous test. The shape of a single detected PD pulse is presented in Fig. 8.

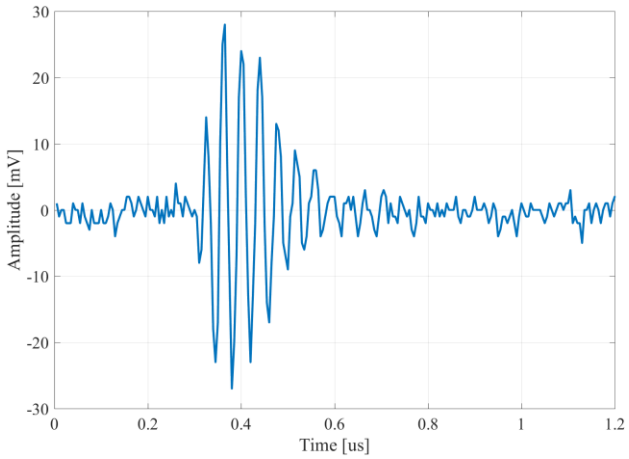

Fig. 8. Acquired PD pulse during the test under temperature difference.

The time variation of the PDRR during the test is illustrated in Fig. 9. The PD peaks at 1, 7, 11 mins are related to the effect of the variation of the voltage between 0-10 kV, 10-15 kV and 15-20 kV, respectively. PDs registered at 17 mins are associated with the voltage decrease from 20 kV to 0 kV.

As can be seen, unlike the previous case in Fig. 6, an intensive PD activity during the stationary value of 20 kV is prevalent in respect to the discharges occurring during the voltage variation from different levels. However, by observing both Figs. 6 and 9, one may notice the strong effect of the

thermal stress on the PD activity. Thus, the maximum PDRR value in Fig. 6 was 6 events/mins whereas more than 250 events/mins appeared in the case of elevated temperature. For all the PD events detected and reported in Fig. 9, their amplitude distribution has also been acquired and illustrated in Fig.10. The greatest number of PD events has an amplitude in the range of 20-60 mV, therefore with an average magnitude of around 40 mV, similar to the previous case. This means that the effect of the thermal gradient manifests itself mainly as the increment of the PDRR, but not the PD amplitude.

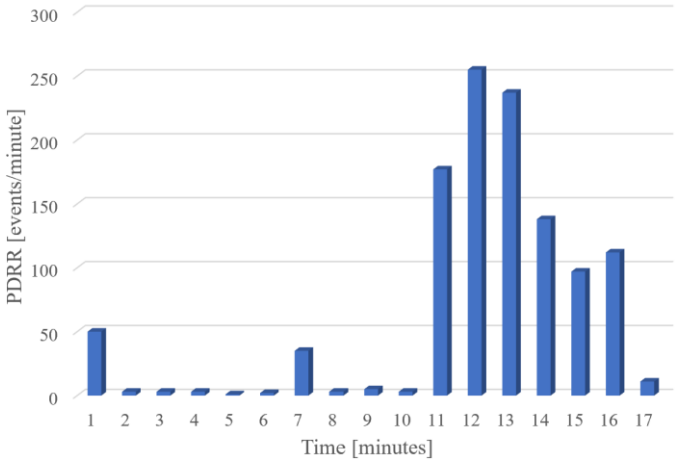

Fig. 9. Trend of the PDRR related to the experimental under temperature difference.

In this paper, tests with only positive polarity voltage have been carried out. However, the voltage polarity does not influence the waveforms of recorded voltage pulses and their amplitude-time parameters because these factors mainly depend on the pulse propagation path. The only parameter that can be changes under negative voltage polarity is the PDIV. In fact, in a previous paper [14] it was observed that, for the same defected specimen configuration adopted in this work and subjected to a DC stress, the PDIV resulted lower than that detected under positive polarity of about the 20%.

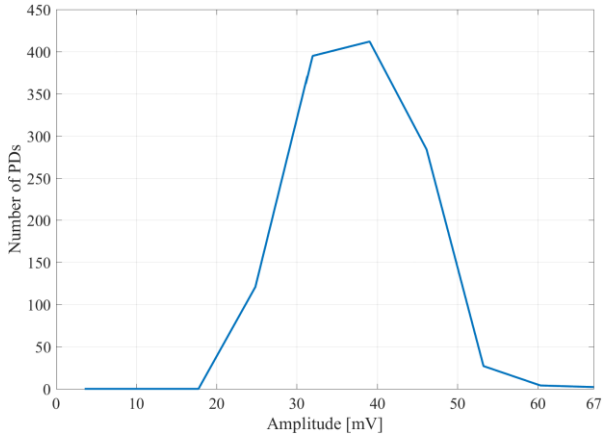

Fig. 10. Amplitude distribution of the PD signals acquired in the test under temperature difference.

IV. The Developed Simulation Model

To provide a comprehensive explanation for the experimental observations and to elucidate involved physical processes, a simulation model has been developed. The model is implemented in Matlab environment, with the aim to provide useful information regarding how the PD behavior changes under DC stress.

The main important and innovative element proposed by this model concerns the possibility to carry out simulations also when applying different temperatures to the samples. The model is an extension of the "three-capacitor model" (sometimes called abc-model), which is traditionally used to simulate the PD behavior under AC stress in dielectrics containing an air void, see e.g. [15] for a recent review. During the years, starting from the three-capacitor model, different circuit structures for different simulation aims and for different specimen configurations have been proposed. The various types of circuit simulation models present in literature were collected and described in a review paper published by Cheng Pan *et al* in 2019 [16]. One advantage with macro models based on circuit approach is the considerably shorter simulation time. However, to obtain reliable results, measured data from the test setup are needed. For the purposes of the present study, the original structure comprised of resistors and capacitors [15]-[17] is modified by replacing the constant resistors, representing the conductivity of the dielectric layers, by variable value resistors defined by the temperature and the electric field values. For the resistor resembling the air-filled void, two different values are used, both estimated from the calculated electric field within the cavity corresponding to PD inception and extinction voltages.

The equivalent circuit in Fig. 11 represents the connection of the specimens depicted in Fig. 12, where resistor *Ra* and capacitor *Ca* are referred to the healthy specimen, whereas *Rb*, *Rc*, *Rd* and *Cb*, *Cc* and *Cd* are introduced for the specimen containing the defect.

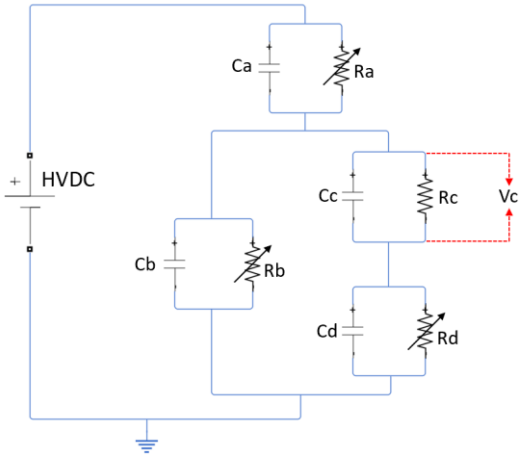

Fig. 11. Equivalent electrical circuit of the two specimens in series connected.

The values of the capacitances, depending on the samples geometry and material properties are equal to *Ca*=60.0 pF,

Cb=49.5 pF, *Cc*=0.37 pF and *Cd*=1.00 pF.

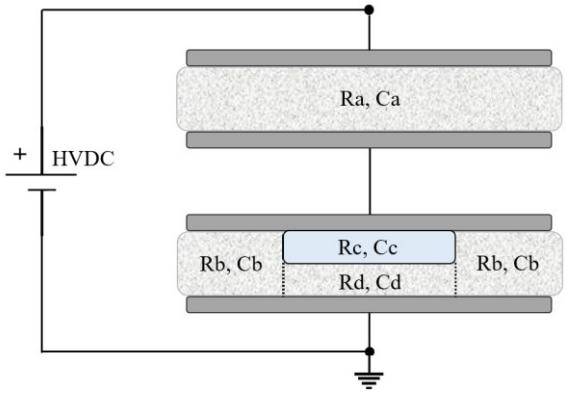

Fig. 12. Electrical parameters associated to the two specimens.

The values of the resistors *Ra*, *Rb* and *Rd* were calculated as $R = L/\sigma S$ using material conductivity σ_{XLPE}, thickness L and area S of the specimens' layers. The values of L and the diameters of each specimens' layers are indicated in Fig. 2. The electrical conductivity was obtained using (1), accounting for the local electric field strength E and temperature T [18].

$$\sigma_{XLPE} = A \cdot exp^{\left(\frac{-\varphi \cdot q}{k_b \cdot T}\right)} \cdot \frac{\sinh(B \cdot E)}{|E|} \quad (1)$$

Here, the material dependent parameter $A = 8.15 \cdot 10^6$ V/(Ω·m^2), the thermal activation energy $\varphi = 0.78$ eV, and the field constant $B = 1.4 \cdot 10^{-7}$ m/V [19]. The other parameters in the (1), are the elementary charge q, the Boltzmann's constant k_b and the modulus of the electric field E. The capacitances of the equivalent circuit are calculated considering the geometrical properties as lumped components and assuming constant permittivities of the gas and the dielectric.

In the original model, each element in the circuit has a fixed value calculated based on the physical and geometric parameters of the specimen [16]-[17]. In the proposed model, the resistance of the cavity *Rc* has been set by considering the conductivity value of the gas embedded within the defect. In particular, two different values were assigned for the gas conductivity σ_g as indicated in Table I, depending on the electric field value E_{cavity} within the air void and E_{inc} if PD events are not present, or E_{ext} if PDs are triggered (here, E_{inc} and E_{ext} are the values of the electric field within the air void corresponding to inception and extinction of the PD activity).

TABLE I.

Different values of σ_g, used to calculate R_c, based on the comparison between E_{cavity} with E_{inc} and E_{ext}.

σ_g [S\m]	E_{cavity}	
10^{-15}	$< E_{inc}$	In absence of PD
10^{-4}	$\geq E_{inc}$	
10^{-15}	$< E_{ext}$	In presence of PD
10^{-4}	$\geq E_{ext}$	

The Paschen's law is used to determine the E_{inc} which was fixed around 5 kV/mm and thus, for the 0.3 mm defect layer corresponds to a PDIV of 1.5 kV. Whereas, the value of E_{ext} is fixed to 1 kV/mm [20]. Respectively, the resistor *Rc* was assigned to two different values corresponding to the state before and after the occurrence of each discharge. The calculated values of individual resistors of the proposed equivalent scheme, before and during the inception of PD and for both thermal conditions are listed in Table II.

TABLE II

Calculated values of the equivalent electrical circuit resistors, before and during the PD inception for both thermal conditions.

Circuit element	Both samples at 20 °C		Healthy sample at 80°C Defected sample at 20°C	
	Before PD	During PD	Before PD	During PD
Ra [Ω]	$1.00 \cdot 10^{13}$	$9.89 \cdot 10^{12}$	$5.33 \cdot 10^{10}$	$5.23 \cdot 10^{10}$
Rb [Ω]	$1.22 \cdot 10^{13}$	$1.20 \cdot 10^{13}$	$1.22 \cdot 10^{13}$	$1.20 \cdot 10^{13}$
Rc [Ω]	$2.39 \cdot 10^{16}$	$2.39 \cdot 10^{5}$	$2.39 \cdot 10^{16}$	$2.39 \cdot 10^{5}$
Rd [Ω]	$6.08 \cdot 10^{14}$	$6.05 \cdot 10^{14}$	$6.08 \cdot 10^{14}$	$6.05 \cdot 10^{14}$

The model has been implemented in Matlab to solve discretized differential equations for the nodal voltages in the equivalent circuit. In the simulations, the time step has been set to 0.1 μs taking into account the time interval between two subsequent discharges such that, in the simulation, the PDRR was in accordance with the measured PDRR.

V. Simulation Results

A. Specimens at Room Temperature

The measurement conditions of the first test, in which both specimens are kept at the same temperature, was first implemented into the model. The voltage was applied according to the diagram in Fig. 4, and the circuit parameters were obtained using σ_g and σ_{XLPE} as described above.

In Fig. 13, the PDRR distribution obtained from the simulations (in orange colour) is compared with the experimentally obtained distribution (in blue colour). Although the simulated PDRR values do not exactly match the experimental data, a certain similarity and trends can be recognized. In particular, one may notice in the experimental results that the number of discharges in the first 10 minutes after voltage application (at 10 kV and 15 kV, Fig. 4) is lower compared to what is detected when the voltage raised to 20 kV. Similar trend can be observed also in the simulations.

Moreover, from the developed model, it is also possible to estimate the voltage variations across the cavity, which is shown in Fig. 14. As seen, it starts from zero value and increases exponentially tending towards an asymptotic value.

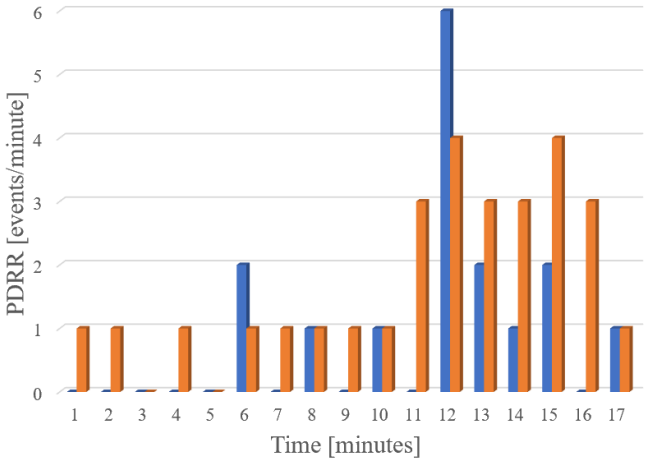

Fig. 13. Trend of the PDRR related to the simulation (orange color) and experimental (blue color) results in which both specimens are kept at room temperature.

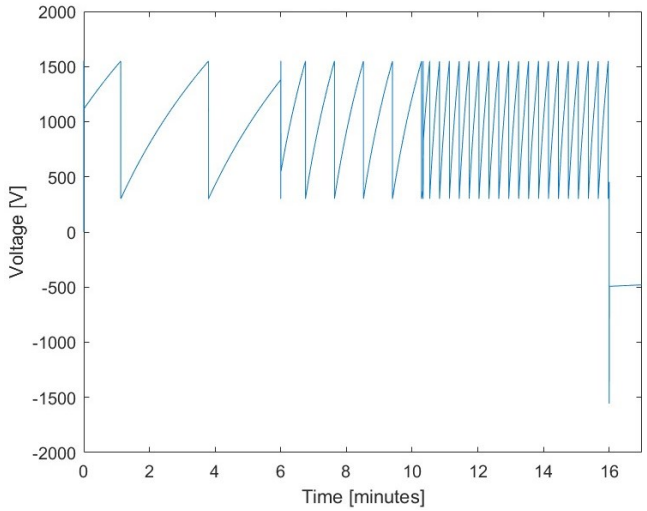

Fig. 14. Voltage applied to the cavity in the simulation test at room temperature.

As soon as a PD is triggered at approximately 1500 V (estimated from the Paschen law), the voltage across the cavity drops to 300 V. Then, due the externally applied DC stress, the voltage within the cavity starts to increase again and then is reduced to 300 V at the next PD event in a repeating process. Using the voltage variation depicted in Fig. 4, it is possible to estimate variable voltages across the entire dielectric layers. Considering that the electric field inside each region (represented by corresponding resistor in the circuit) is dependent on the total voltage varying over time, the value of the equivalent resistors must be update at each time step. In other words, the variable resistors introduced in the developed model have a value depending on the temperature and the voltage applied to each resistor. Since the latter is affected not only by the applied voltage but also PD activity, it can then be stated that the modeled problem is clearly not linear.

The time variation of the charge associated with PD activity obtained by integrating the discharge current over time is presented in Fig. 15. As can be seen, a charge of +1634 pC is involved in each PD event at high voltage level. When the applied voltage is switched off and reduced from 20 kV to 0 kV, the negative charge of -1634 pC is released from the system.

Based on the above, the developed simulation model is capable to provide useful information related to the principal PD behaviour in insulating materials subjected to the DC and thermal stresses. Further improvements are needed to bring the simulated results closer to the experimental ones.

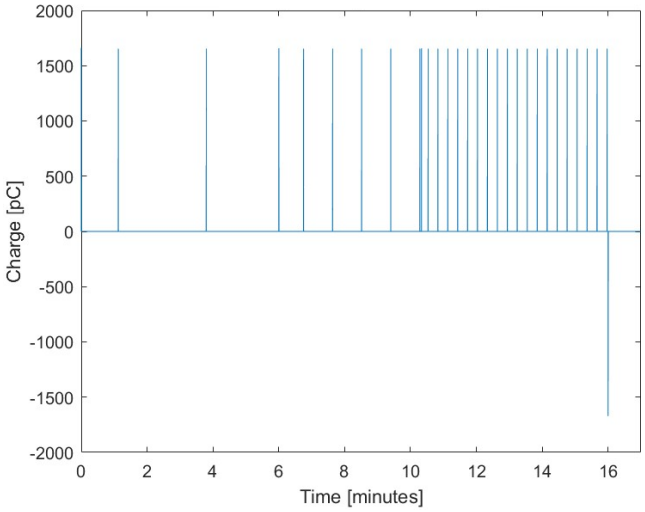

Fig. 15. Charge through to the cavity in the simulation test at room temperature.

B. Specimens Under Temperature Difference

In the next study, the temperature difference was introduced between the two specimens, applying the same simulation conditions as for the previous case when both specimens were kept at the same temperature. As explained in section IV, in this case, the temperature variation affects the electric conductivity and thus the values of *Ra*, *Rb* and *Rd*, which are updated each 0.1 μs in the simulation time. The value of *Rc* is continuously calculated on the basis of the σ_g value presented in Table I, like for the previous case.

The simulated PDRR distribution is reported in Fig. 16, together with the experimental results presented earlier (blue color). As seen, the computed numbers of discharges are slightly different from the measured values, but the trend of the PDRR variations is very similar for both simulated and experimental results. The differences in PDRR magnitudes can be attributed to the fact that in the experimental test, a certain number of discharges has been filtered out by the Pry-Cam acquisition software and some PD events have not been probably detected because their magnitude was below the noise threshold. Nevertheless, a good performance of the developed model can be noticed by considering the fact that the PDRR values under thermal stress are greater compared to those

obtained from the simulations and tests with the specimens kept at the same temperature.

By comparing Figs. 13 and 16, it is evident that without the thermal effect, the PDs due to the voltage variation (dv/dt for the different voltage levels) prevail over those detected during the time interval of constant applied voltage. The discharge behaviour is opposite when temperature variation is introduced.

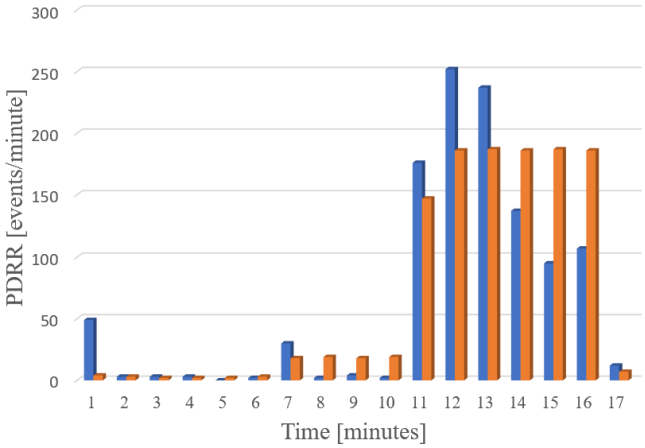

Fig. 16. Trend of the PDRR related to the simulation (orange color) and experimental (blue color) results in which the specimens are subjected to the temperature difference.

In Figs. 17 and 18, the voltage applied to the cavity and the charge through to the cavity associated to the PDs are reported.

As can be seen, the voltage within the cavity exposed to thermal stress undergoes multiple variations due to the greater number of discharge events (compare Fig. 17 with Fig. 14). However, as can be observed in Figs. 15 and 18, the amount of the charge through the cavity is the same in both test conditions due to the fact the PD inception/extinction parameters remained unchanged.

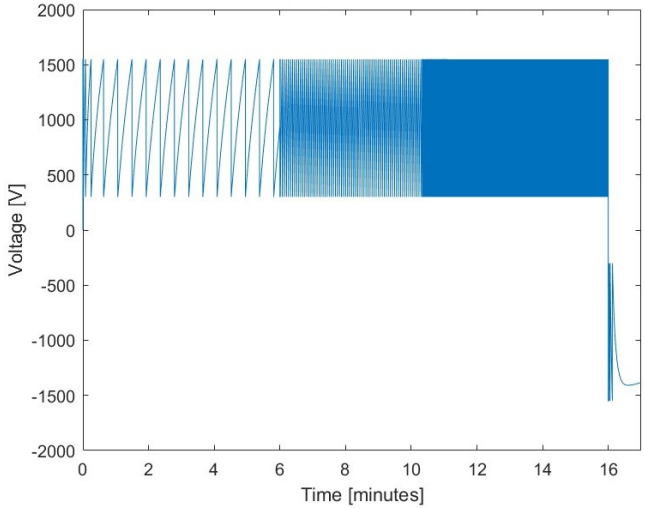

Fig. 17. Voltage applied to the cavity in the simulation test with temperature difference.

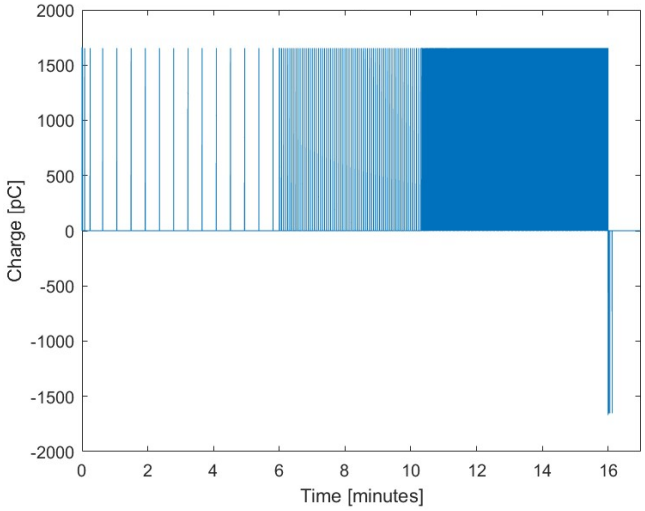

Fig. 18. Charge through to the cavity in the simulation test with temperature difference.

VI. Conclusions

The proposed work explores the PD phenomenon under DC voltage stress. The effect of thermal gradient in the insulation has been investigated by using the novel experimental setup allowing to imitate it in a "discrete" manner thus reproducing the behavior of a defected cable insulation. The setup contained two material samples, one healthy and one with the defect, connected in series and kept at either equal or at different temperatures. In both cases, the defected sample is kept at room temperature to distinguish the role of the temperature difference from the influence of the absolute temperature. The experimental results show the evident increase of the PD activity when the two samples are subjected to different temperatures. This is attributed to the fact that under thermal gradient resulting in different conductivities of the two samples, the applied voltage is unequally split between them causing stronger field in the defect thus promoting the inception of PDs. This also implies that the PD activity in a defect in the insulation of an HVDC cable depends on the location of the cavity and the radial temperature gradient over the dielectric layer.

To theoretically support the obtained experimental results, a simulation model of the novel experimental setup has been developed. It is based on a macroscopic conductivity model approach of the dielectric layers. The conducted simulations provided the PDRR, the time variations of the voltage on the defect and the charge through it. The results of the simulations follow qualitatively the experimental ones for both tests. The observed discrepancies are explained by various factors, e.g. due to ignoring some discharges of lower amplitude by the trigger level denoising procedure used in the measurement system. Also, limitations of the model must be considered. In particular, the oil temperature is assumed to be constant in the model during the entire PD test. In reality, despite of the rather test duration 17 minutes, the oil temperature was decreasing over time and it was not monitored to minimize the impact of the sensors in the setup. In addition, the resistance of the defect in the model was calculated based on air properties. Unlike the case in AC, where

the PD phenomenon is driven by the capacities of the dielectric and the defect, under DC voltage, the value of the electric field inside a cavity depends on the resistivities. Because the roughness of the cavity surface, high electric field levels can be reached locally. This leads to relatively high currents towards the direction of the electric field that can drain the charges accumulated at the main surfaces of the cavity, in proximity of the edges. For this reason, a more accurate estimation of the equivalent resistance of the cavity should consider both the contribution of the air bulk resistivity as well as that of the cavity' surface. The latter can be affected by the enhanced PD activity over time, which can heal the cavity walls and therefore change their resistance. However, this aspect should be considered experimentally, and it will be taken into account in the next version of the simulation model. Further limitation is that each occurring PD assumes the whole defect being discharged, something that will introduce uncertainties for larger defect volumes.

In summary, the present work proposes a new measurement setup for PD analysis under DC stress and thermal gradient as well as a novel simulation model useful to predict the PD activity which considers the conductivity variation with the temperature and electric field. However, further improvements of the model are still needed. In future works, an update of the model will be presented. Furthermore, PD tests will be made in a model cable to compare the measurement results with those obtained in the present work, where the two specimens have been used.

ACKNOWLEDGMENT

This work was realized with the co-financing from European Union – FSE, PON Research and Innovation 2014-2020 – DM 1062/2021.

REFERENCES

[1] P. Morshuis, A. Cavallini, D. Fabiani, G. C. Montanari and C. Azcarraga, "Stress conditions in HVDC equipment and routes to in service failure," in *IEEE Transactions on Dielectrics and Electrical Insulation*, vol. 22, no. 1, pp. 81-91, Feb. 2015, doi: 10.1109/TDEI.2014.004815.

[2] G. C. Montanari, "Bringing an insulation to failure: the role of space charge," in *IEEE Transactions on Dielectrics and Electrical Insulation*, vol. 18, no. 2, pp. 339-364, April 2011, doi: 10.1109/TDEI.2011.5739438.

[3] T. Hammarström and S. M. Gubanski, "Detection of Electrical Tree Formation in XLPE Insulation through Applying Disturbed DC Waveforms," in *IEEE Transactions on Dielectrics and Electrical Insulation*, vol. 28, no. 5, pp. 1669-1676, October 2021, doi: 10.1109/TDEI.2021.009717.

[4] R. Bartnikas, "Partial discharges. Their mechanism, detection and measurement," in *IEEE Transactions on Dielectrics and Electrical Insulation*, vol. 9, no. 5, pp. 763-808, Oct. 2002, doi: 10.1109/TDEI.2002.1038663.

[5] U. Fromm, "Interpretation of partial discharges at DC voltages," *IEEE transactions on Dielectrics and Electrical Insulation*, vol. 2, no. 5, pp. 761–770, 1995, doi: 10.1109/94.469972

[6] P. H. F. Morshuis and J. J. Smit, "Partial discharges at DC voltage: their mechanism, detection and analysis," in *IEEE Transactions on Dielectrics and Electrical Insulation*, vol. 12, no. 2, pp. 328-340, April 2005, doi: 10.1109/TDEI.2005.1430401.

[7] G. Rizzo, P. Romano, A. Imburgia and G. Ala, "Partial Discharges in HVDC Cables - The Effect of the Temperature Gradient During Load Transients," in *IEEE Transactions on Dielectrics and Electrical Insulation*, vol. 28, no. 5, pp. 1767-1774, October 2021, doi: 10.1109/TDEI.2021.009602.

[8] P. Romano, G. Presti, A. Imburgia and R. Candela, "A new approach to partial discharge detection under DC voltage," in *IEEE Electrical Insulation Magazine*, vol. 34, no. 4, pp. 32-41, July-August 2018, doi: 10.1109/MEI.2018.8430041.

[9] G. Rizzo, P. Romano, A. Imburgia, F. Viola, G. Schettino, G. Giglia and G. Ala, "Effect of Heat Exchange Transient Conditions With Moving Water-Air Interface on Space Charge Accumulation in Undersea HVdc Cables," in *IEEE Transactions on Industry Applications*, vol. 57, no. 5, pp. 4528-4536, Sept.-Oct. 2021, doi: 10.1109/TIA.2021.3099087.

[10] G. Rizzo, P. Romano, A. Imburgia, F. Viola, and G. Ala, "The Effect of the Axial Heat Transfer on Space Charge Accumulation Phenomena in HVDC Cables," *Energies*, vol. 13, no. 18, p. 4827, Sep. 2020, doi: 10.3390/en13184827.

[11] G. Rizzo, T. J. Å. Hammarström, A. Imburgia, P. Romano, G. Ala and Y. V. Serdyuk, "Characteristics of partial discharges in an experimental setup reproducing HVDC cable insulation operating conditions," *2021 IEEE Conference on Electrical Insulation and Dielectric Phenomena (CEIDP)*, 2021, pp. 191-194, doi: 10.1109/CEIDP50766.2021.9705421.

[12] P. Romano, A. Imburgia and G. Ala, "Partial discharge detection using a spherical electromagnetic sensor" *Sensors*, vol. 19, no. 5, 2019, https://doi.org/10.3390/s19051014

[13] A. Imburgia, A. D. Fatta, P. Romano, G. Rizzo, V. L. Vigni and G. Ala, "A Study on Partial Discharges Pattern Recognition Under DC Voltage Through Clustering Algorithms and Cross Correlation Filter," in IEEE Transactions on Dielectrics and Electrical Insulation, vol. 30, no. 6, pp. 2543-2550, Dec. 2023, doi: 10.1109/TDEI.2023.3308532.

[14] P. Romano, A. Imburgia, G. Rizzo, G. Ala and R. Candela, "A New Approach to Partial Discharge Detection Under DC Voltage: Application to Different Materials," in IEEE Electrical Insulation Magazine, vol. 37, no. 2, pp. 18-32, March-April 2021, doi: 10.1109/MEI.2021.9352713.

[15] Z. Achillides, G. E. Georghiou and E. Kyriakides, "Partial discharges and associated transients: the induced charge concept versus capacitive modeling," in *IEEE Transactions on Dielectrics and Electrical Insulation*, vol. 15, no. 6, pp. 1507-1516, December 2008, doi: 10.1109/TDEI.2008.4712652.

[16] C. Pan, G. Chen, J. Tang and K. Wu, "Numerical modeling of partial discharges in a solid dielectric-bounded cavity: A review," in *IEEE Transactions on Dielectrics and Electrical Insulation*, vol. 26, no. 3, pp. 981-1000, June 2019, doi: 10.1109/TDEI.2019.007945.

[17] T. S. Negm, M. Refaey and A. A. Hossam-Eldin, "Modeling and simulation of internal Partial Discharges in solid dielectrics under variable applied frequencies," *2016 Eighteenth International Middle East Power Systems Conference (MEPCON)*, Cairo, Egypt, 2016, pp. 639-644, doi: 10.1109/MEPCON.2016.7836959.

[18] N. Adi, T. T. N. Vu, G. Teyssèdre, F. Baudoin and N. Sinisuka, "DC Model Cable under Polarity Inversion and Thermal Gradient: Build-Up of Design-Related Space Charge"; *Technologies* 2017, 5, 46. https://doi.org/10.3390/technologies5030046

[19] Y. Qin, N. Shang, M. Chi and X. Wang, "Impacts of temperature on the distribution of electric-field in HVDC cable joint," 2015 *IEEE 11th International Conference on the Properties and Applications of Dielectric Materials* (ICPADM), Sydney, NSW, Australia, 2015, pp. 224-227, doi: 10.1109/ICPADM.2015.7295249.

[20] R. Schifani, R. Candela and P. Romano, "On PD mechanisms at high temperature in voids included in an epoxy resin," in IEEE Transactions on Dielectrics and Electrical Insulation, vol. 8, no. 4, pp. 589-597, Aug. 2001, doi: 10.1109/94.946711.